SNR Enhancement By DWT For Improving The Performance Of Φ-OTDR In Vibration Sensing

Atubga David Atia Ibrahim, Khushnood Abbas, Bonny Ernestina Linda

Key Lab of Optical Fiber Sensing and Communication(Ministry of Education), School of Information and Communication Engineering, University of Electronic Science and Technology of China, UESTC, Chengdu 611731, ,
atubgadavid@ymail.com

Department of Computer Science, Zhoukou Normal University, Henan, China. Pin:466001
khushnood.abbas@gmail.com

School of Management Science and Economics, University of Electronic Science and Technology of China, UESTC, Chengdu, 611731, Sichuan, China.
elbonnym@yahoo.com

Abstract: The distributed optical vibration sensors (DOVS) have been extensively investigated with regards to their significant impact in sensor applications. The Phase-sensitive Optical Time Domain Reflectometry (Φ-OTDR) which is one of the most distinguished distributed optical fiber sensing technologies has lately attracted enormous research attention due to its merits of high precision measurements, fast speed response, long perimeter monitoring, capabilities in vibration detection abilities, among others. However, it becomes very stressful when data meant for the said sensing technology in vibration detection is impeded by harsh environmental conditions. Therefore, in order to successfully enhance effective vibration detection by the Φ-OTDR sensing technology, noise filtering becomes very crucial. As a result, we executed Hilbert transform to first retrieve both the real and imaginary parts of the complex signal of the Φ-OTDR sensing data. Then a discrete wavelet transform (DWT) was identified and carefully applied to achieve the denoised results. We further performed angle and phase unwrapping for the vibration detection. In the experiment, the Signal-Noise-Ratio (SNR) of the location information is greatly improved from 16.2 dB to 30.2 dB on a 3km sensing fiber range. The proposed method has the potentials of precisely extract intrusion location from any strong noise background. As proof of concept, the theoretical and experimental setup are equally presented.

Keywords: Phase-sensitive Optical Time Domain Reflectometry (Φ-OTDR), Discrete Wavelet Transform (DWT), Signal-to-Noise-Ratio (SNR)

1. Introduction

Distributed optical fiber sensing (DOFS) technologies have been widely explored in recent decades of which vibration sensing based on Phase-sensitive Optical Time Domain Reflectometry (Φ-OTDR) has become the focal point. The said sensing technology has since contributed significantly and have attracted great research attention due to its merits of fast speed response [1], high sensitivity, large dynamic range sensing and high positioning accuracy [2], among others. Also, the Φ-OTDR has proved proficient, effective and the ultimate of detecting and locating one or more vibration events occurring at any position along the sensing fiber [3]. In addition, a reflectometry using a 90o optical hybrid successfully achieved homodyne detection [4], whereas phase information of Rayleigh scattered light wave in optical fiber equally demonstrated of been capable of transforming a fiber cable into a massive sensor array in distributed acoustic sensing (DAS) [5]. Additionally, the application of single mode fiber (SMF) on a truly distributed optical vibration sensor based on Φ-OTDR was successfully demonstrated for vibration detection [6]. Notwithstanding, one key advantage of using the Φ-OTDR in distributed sensing is that the signal-to-noise ratio (SNR) for locating the external vibration is relatively high [7], [8]. Consequently, vibration detection can only be successful if data meant for vibration detection is void of noise and other distortions. As a result, a considerable number of signal denoising techniques have been demonstrated including bilateral filter, wavelet with bayes-shrink thresholding [9], median filtering [10], Kalman filtering [11], correlation and moving average [12], curvelet transform [13], empirical mode decomposition (EMD) [14], among others. However, these traditional methods come with inherent weaknesses such that they are considered not suitable in cases where signals often overlap the noise at many frequency bands [15], [16]. Constructively, per the drawbacks of the preceding denoising methods, the strength of each technique largely depends on the kind and source of data. Although the said techniques might be good for denoising in same orientation, the integrated discrete wavelet transform approach worked perfectly in our case and considered the desired option. Hence in this paper, the original Φ-OTDR signal was first processed by using Hilbert transform to successfully retrieve both the real and the imaginary parts of the complex signal. Then the integrated discrete wavelet transform was explored and applied using desired decomposition level which successfully denoised the said signals. Finally, we carried out angle and phase unwrapping, differential phase extraction to reveal the vibration point. The experimental results by the proposed technique heightened the vibration point with a significant enhancement of the SNR value from 16.2 dB to 30.2 dB. The next section introduces the basis of the discrete wavelet transform whereas the presentation of the proposed method is represented in Section 3, with Section 4 illustrating the experimental setup of the Φ OTDR sensing system including discussions of results and finally, Section 5 concludes the paper.

2. Theoretical Basis Of The Φ-OTDR Sensing System

2.1 Basic principles of Φ-OTDR sensing system

The Φ-OTDR system which is the OTDR prototype was initially demonstrated by Henry F. Taylor in 1993 [17]. It has since noted as one of the key distributed optical fiber sensing technologies [18]. Traditionally, the working principle of the two systems is related, and compared to the broadband light source used by the conventional OTDR system, the Φ-OTDR system uses ultranarrow linewidth lasers as its main source of light. It receives and uses the interference effect between the

backward Rayleigh light in the wide pulse, then injects the high coherent light into the sensing fiber and the reflected coherent Rayleigh scattered light is detected by the detector [18]. The Φ-OTDR system has the advantage of high sensitivity as well as a longer distance sensing ability. Apparently, the Φ-OTDR can principally enhance direct detection and coherent detection of two structures. These attributes are the main difference between the two systems [18]. Significantly, the advantage of direct detection by the Φ-OTDR system is known to be relatively low in terms of cost. Also, its data processing method and structure are quite simple. The main disadvantage of coherent detection for the Φ-OTDR system is the strict requirement on the coherence of light source [18]. In the orientation of Φ-OTDR system when there is perturbation on the fiber as illustrated above, at a certain point the internal refractive index and length of the fifiber at that location will change, resulting in a change in the optical phase of the optical interference [18]. This change therefore leads to backward Rayleigh scattering light intensity, which means that the backward optical power changes and will be disturbed when the scattering power curve subtracts the power curve without disturbance. An illustration of the working principle of the Φ-OTDR system is hereby presented in Figure 1

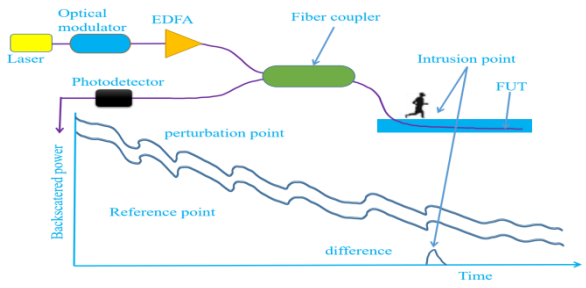

Fig. 2. *Basic principles of Φ-OTDR sensing system*

3. The proposed DWT for Vibration detection

3.1 The retrieval of the complex signal

To effectively carry out the denoising processes, we applied Hilbert transform for demodulation to first retrieve the complex signal of which further processing for the enhancement of both the real part and the imaginary part of the signal could be obtained by the application of Eq. (1) as presented below.

$$q(\iota) = h\lfloor I(\iota)\rfloor \quad (1)$$

where $h\lfloor I(\iota)\rfloor$ represents Hilbert transform and $q(\iota)$ could successfully be retrieved. Hence to successfully obtain the real and imaginary parts of the complex signal, we applied Eq. (2).

$$y = I(\iota) + jq(\iota) \quad (2)$$

where y is the complex signal, the $I(\iota)$ is the real signal and $q(\iota)$ represents the imaginary signal. This was then followed by the proposed denoising approach presented in the next section.

3.2 The basis of the Discrete Wavelet Transform

The Discrete Wavelet Transform (DWT) is capable of transforming the discrete time signal into discrete wavelet representations [19]. It transforms the input signal into the series of low pass and a high pass series of wavelet coefficients. In DWT, there are many wavelet families that are applied for data processing of which these include the; Haar, Daubechies, Symlet filtering, among others. A successfully implementation of these families is greatly achieved by appropriately selecting the desired thresholding scheme.

3.3 Thresholding techniques in Discrete Wavelet Transform

The discrete wavelet transform (DWT) is implemented by the application of discrete sets of wavelet scales and translations to successfully harness effective signal processing while obeying some defined principles. A remarkable fact about the DWT is that it is represented as a mathematical microscope and time-frequency approach used for the analysis of signals after decomposing them over dilated and translated wavelets structures [21]. Mathematically, a wavelet is expressed as a function φ which belongs to $L^2(R)$ with a zero [21], as presented below in Eq. (3);

$$\int_{-a}^{a} \phi(t)dt = 0 \quad (3)$$

This process decomposes the signal into an orthogonal set of wavelets components and by thresholding the said components, the denoised signal is obtained. The standard wavelet thresholding techniques mainly consists of hard thresholding and soft thresholding functions [21]. In wavelet transformation, threshold selection is very essential. Therefore if the threshold value is too small or large it leads to inaccurate estimation [21]. Here, we present the two key thresdholding techniques to include the soft and hard thresholding schemes [21] of which the soft thresdholding is expressed as presented in Eq. (4) below;

$$\hat{x} = \begin{cases} y - \mathrm{sgn}(y)T & if\ |y| \geq T \\ 0 & if\ |y| < T \end{cases} \quad (4)$$

On the other hand, the hard thresdholding which is also known as the keep or kill approach is expressed as;

$$\hat{x} = \begin{cases} y & if\ |y| \geq T \\ 0 & if\ |y| < T \end{cases} \quad (5)$$

In applying either of the thresdholding techniques, the levels of the received signal are separated by the wavelet transform of which the received signal coefficients are computed to the desired state. The variance (σ^2) of the noise is calculated using the wavelet coefficients as presented below;

$$\hat{\sigma} = \frac{med(|W_{j,k}|)}{0.6745} \quad (6)$$

where *med(.)* indicates the median. The thresdhold value is then calculated using the variance as presented below.

$$T = \sigma\sqrt{2log(n)} \quad (7)$$

Of which *T* is the thresdhold value an *n* is the length of the signal. In this article, Eq. (7) is applied to enhance effective results. The original signal is then reconstructed perfectly using the inverse discrete wavelet transform and retained coefficients. The coefficient is then set to zero if it is smaller than the threshold value. The denoised signal at this point is recovered by performing inverse DWT on the results. Therefore, the wavelet is constructed from a scaling function

that describes its scaling features by capturing both the frequency and location information as expressed in Eq. (8) and (9) respectively;

$$W_{\varphi(x_0,y)} = \frac{1}{\sqrt{P}} \sum_q f[n] \varphi_{x,y}[n] \quad for\ x \geq x_0 \tag{8}$$

$$W_{\varphi(x_0,y)} = \frac{1}{\sqrt{P}} \sum_q f[n] \varphi_{x,y}[n] \tag{9}$$

where $\varphi_{(x_0,y)}[n]$ and $\varphi_{x,y}[n]$ represent the sampled forms of the basic functions $\varphi_{(x_0,y)}[f]$ and $\varphi_{x,y}[f]$. In accordance with the inverse form of DWT, it can also be expressed as demonstrated in Eq. (10) below;

$$f[n] = \frac{1}{\sqrt{m}} \sum_y \varphi_\varphi(x_0, y)[n] \tag{10}$$
$$= \frac{1}{\sqrt{m}} \sum_{x=x_0} \sum_y \varphi_\varphi(x_0, y) \varphi_{x_0,y}[n]$$

where $f(n), \varphi_{x_0,y}(n)$ and $\varphi_{x,y}(n)$ are considered as discrete functions defined in $(0, M\text{-}1)$, totally M points, because the sets $\{\varphi_{x_0,y}[n]\} b \in R$ and $\{\varphi_{x,y}[n]\}\ xy \in R2, x \geq 0$ are orthogonal to each other. Here we can simply take the inner product to obtain the wavelet coefficients as illustrated in Eq. (8) called the approximation coefficients and in Eq. (9) expressed as the detailed coefficients. On the other hand, the computational analysis of the symlet function s_φ involving the discrete wavelet transform is presented as follows;

$$\phi_{x,y}[n] = 2^{x/2} \phi\left[2^x n - y\right] \tag{11}$$
$$\sum_n s_\phi[n'] \sqrt{2} \phi\left[2(2^x n - y) n'\right]$$

Therefore when $n' = m - 2y$, this can further be expressed as;

$$\phi_{x,y}[n] = \sum_m \phi[m - 2y] \sqrt{2} \phi\left[2^{x+1} n - m\right] \tag{12}$$

Hence, by combining the above equations with Eq. (8), it will be illustrated as;

$$\begin{aligned} w_\varphi(x,y) &= \frac{1}{\sqrt{m}} f[n] \phi_{x,y}[n] \\ &= \frac{1}{\sqrt{m}} \sum_n f[n] 2^{x/2} \phi\left[2^x n - y\right] \\ &= \frac{1}{\sqrt{m}} \sum_n f[n] 2^{x/2} \sum_m s\phi[m - 2y] \sqrt{2} \phi\left[2^{x+1} n - m\right] \\ &= \sum_m s_\phi[m - 2y] \left(\frac{1}{\sqrt{m}}\right) \sum_n f[n] 2^{(x+1)/2} \phi\left[2^{(x+1)} n - m\right] \\ &= \sum_m s_\phi[m - 2y] w_\phi[x+1, m] \\ &= s_\phi[-n] * w_\phi[x+1, n] \end{aligned} \tag{13}$$

Therefore, during the denoising process, the detail coefficients can be expressed as shown below in Eq. (14);

$$w_\phi[x, y] = s_\phi[-n] * w_\phi[x+1, n] n = 2y, y \geq 0 \tag{14}$$

As a result, the Φ-OTDR zero-band noisy signal in the denoising process can be viewed as approximation coefficients with order x. That is, $w_\phi[x, y] = w_\phi[x, n]$ where by applying Eq.(13), and (14), the next level of approximation and detail coefficients can be obtained with the desired denoising output.

3.4 The steps involved in the denoising

The presentation of the methodological approach involving the denoising of the Φ-OTDR noisy data for vibration detection is illustrated as presented beneath.

- Load the Φ-OTDR noisy data
- Apply Hilbert Transform
- Perform demodulation to retrieve the complex signal
- Obtain both the real and imaginary noisy signals
- Apply discrete wavelet transform for denoising
- Carefully select appropriate coefficient for the denoising process
- Perform inverse discrete wavelet transform
- Attain the desired denoised imaginary and real signals
- Perform angle and phase unwrapping
- Execute phase extraction
- Carry out differential phase trace
- Perform vibration detection
- Determine performance evaluation on SNR and STD
- Then execute SNR enhancement affirmation

4. Experimental Results and Discussions

4.1 The experimental setup of a hybrid Φ-OTDR System

The experimental setup of the Φ-OTDR system is demonstrated in Figure 2 below. An ultra-narrow-linewidth (100Hz) laser operating at 1550nm is employed as the light source with a 1:99 polarization maintaining (PM) coupler. The laser output is divided into two branches by a 1:99 PM coupler forming a probe light and a local reference light. One of the branches is modulated by In-phase/Quadrature (I/Q) modulator with 500 MHz frequency shift to generate the pulsed probe wave (with 100 ns pulse width, allowing for 10 m spatial resolution). The sampling rate is 2GHz and that of the repetition rate of the probe pulse is 5kHz. The probe pulse is injected into the sensing fiber through a circulator and the Rayleigh scattering (RS) signal is injected into a 90^0 hybrid.

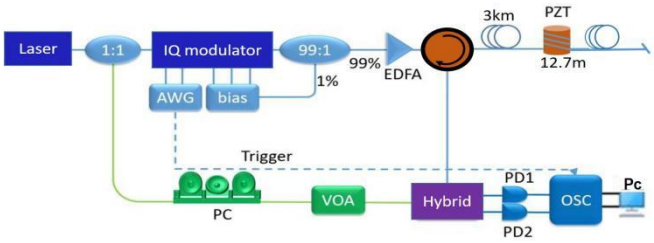

Fig. 2 *The experimental setup of a hybrid Φ-OTDR for vibration detection; I/Q:In phase Quadrature Modulator; EDFA:Erbium-Doped Fiber Amplifier; VOA:Variable Optical Attenuator; PC:Polarization Controller; PD: Photodetector; PZT:Piezo Transducer, Pc:Personal computer*

The 1% branch of the laser output is used as the LO. Before the LO is injected into hybrid, a polarization controller (PC) is inserted in order to match the LO with the selected polarization branch of the hybrid. The two outputs of the hybrid are converted into electrical signals by a two ports AC coupled detector and then sampled by the OSC. At the position of 3km, 12.7m bare fiber is coiled over a cylindrical PZT, used as the test point.The process of phase unwrapping algorithm, signal reconstruction leading to denoising and

vibration point detection on the time domain are completed in real-time with a personal computer.

4.2 Procedure for Vibration Extraction

In order to successfully achieve the vibration detection, both the denoised forms of the real and imaginary parts of the complex signals were retrieved by the application of Eq. (5) which were then smoothly denoised by the application of Eq. (15) and Eq. (16). The denoisied real and imaginary signals were then converted into the magnitude or phase format to facilitate the extraction for the vibration detection by the application of Eq. (16) and (16) respectively below.

$$\alpha(\iota) = \sqrt{y^2(\iota) + h^2[x(\iota)]} \quad (15)$$

We then perform angle ($\angle$) and phase unwrapping as expressed in Eq. (16) below to pave way for the vibration extraction.

$$\in(\iota) = uwp[\angle(I(\iota) + q(\iota))] \quad (16)$$

where $I(\iota)$ and $q(\iota)$ represent both the real and imaginary signals after denoising and then we performed angle and phase unwrapping of the denoised signals harness the retrieval of $\in(\iota)$ for the phase trace. Therefore the angle and phase unwrapping processes aided the vibration detection on the Φ-OTDR signal and its corresponding statistical features.

4.3 Analysis of Results

As previously stated, the retrieval of the complex signal of the Φ-OTDR was performed by applying Hilbert Transform then both the real and imaginary parts of the complex signal successfully achieved by Eq. (6) and Eq. (7) were respectively. Then the DWT denoising technique was carried out by the application of Eq. (14), and Eq. (15) accordingly. The major difference between this approach and our previous work [22] is that the PCA could not process any mid-band signal that was applied. However, this proposed discrete wavelet transform has been able to achieved this task without the performance of any frequency shift and is deemed less stressful. Therefore the original real signal and its denoised signal were then obtained and comparatively demonstrated in Figure 3 (a) and Figure 3 (b) respectively.

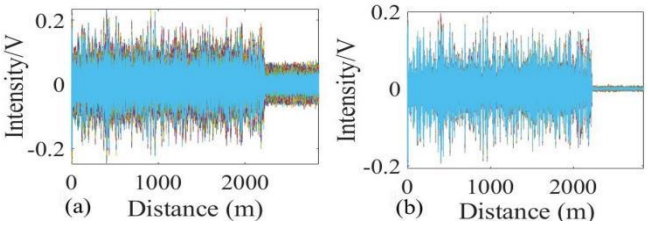

Fig. 3. Illustration of (a) Original noisy signal (b) Denoised signal

In accordance, the representation of the original imaginary and its denoised signal are equally illustrated in Figure 4 (a) and Figure 4 (b) as shown below.

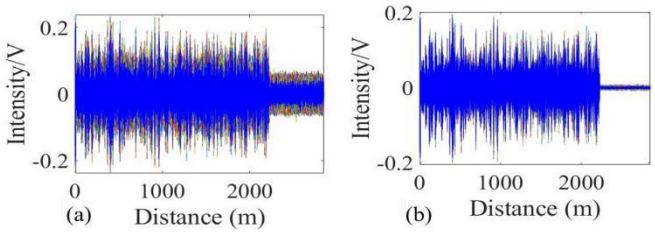

Fig. 4. Illustration of (a) Imaginary noisy signal (b) Denoised imaginary signal

It is very lucid that even though the noise levels seem very scraggy in both original signals, the denoised outputs exhibit a significant level of reduction on the said noise as stated below.

4.4 Vibration point Extraction

A piezoelectric transducer (PZT) with the maximum vibration frequency response of 50 kHz is used as the vibration actuator in the experiment. A single vibration is added to the position of 2100m of sensing fiber. Several series of traces in the Φ − OT DR system were recorded by double channel oscilloscope. The extraction of the phase trace to detect the vibration was then executed soon after obtaining the denoised real and imaginary signals where we performed angle and phase unwrapping by the application of Eq. (15) and Eq. (16) respectively. The reflection of the traces on the signal appears to be very notched due to the presence of much interference and fading phenomenon thereby leading to the existence of extremely low and weak fading points as presented in Figure 5 (a) which is the original signal. Then in contrast, Figure 5 (b) clearly demonstrate the vibration point detected with improved fading points at a distance of approximately 2100m which equally presents a closed view of the said vibration point. Even though the sensing domain, fading posses serious threats in signals processing of which the Phase extraction noise in the differential phase traces sometimes becomes very stressful to precisely locate the vibration zone after denoising. Nevertheless, the proposed model has smoothly enhanced the extraction of the normalised denoised phase trace as demonstrated in Figure 5 (b) below.

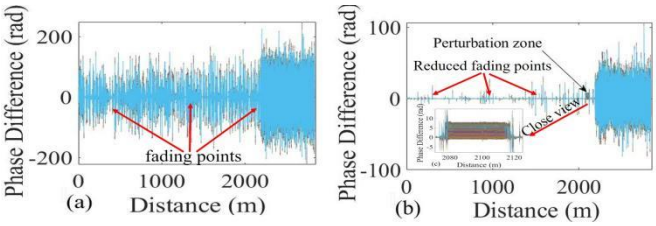

Fig. 5. Illustration of (a) Original phase trace (b) Denoised phase trace

The representation of the original time domain signal and it's denoised form are demonstrated in Figure 6. The red jagged line represents the original data which clearly exhibits extreme level of noise present while the blue thin line also indicates the denoised form of the time domain signal as illustrated below in Figure 6 (a) and Figure 6 (b) respectively.

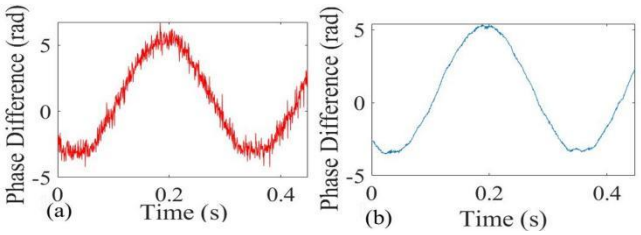

Fig. 6. (a) Original time domain signal (b) Denoised time domain signal

Constructively, the noise level is greatly enhanced per the output of Figure 6 (b). The achievement of the SNR value was then calculated with respect to the time domain signal by the application of Eq. (17) presented beneath.

$$SNR = 10log10\frac{Signal_{power}}{Noise_{power}} \quad (17)$$

The proposed technique effectively obtained an improvement of the SNR value of from 16.2 dB to 30.2 dB corresponding to both the original and denoised signals. Further, the demonstration of the experimental data and the fitted curves are equally shown in Figure 7 of which the blue line represents the experimental data which clearly demonstrates high level of noise present while the red solid line indicates the sinusoidal fitted curve as illustrated in Figure 7

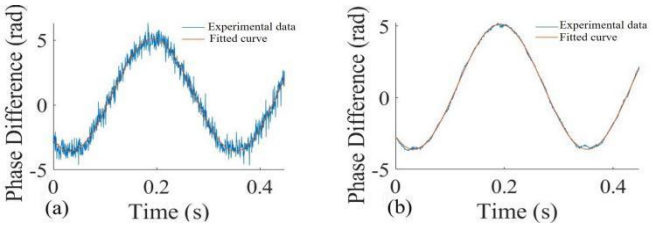

Fig. 7. (a) Experimental and fitted curve (b) Denoised form and fitted curve

(a). Analytically, the noise level is greatly enhanced from the denoised data as presented in Figure 7 (b) beneath. To successfully reassert the SNR enhancement level, the performance of standard deviation (σ) per the said vibration point by applying Eq. (18) and Eq. (19) were executed as respectively presented below.

$$\sigma = \sqrt{var(x-y)} \quad (18)$$

where x represents the noisy signal and y also signifying the cleaned signal. We obtained 0.4670 and 0.0934 as the values of the standard deviation corresponding to the original signal and the denoised signal respectively. The proof of the SNR enhancement is equally authenticated by applying Eq. (19) as shown beneath.

$$\Delta SNR = 10log10\left(\frac{\sigma^2_{Noisysignal}}{\sigma^2_{Denoisedsignal}}\right) \quad (19)$$

Then a final value of 14.0 dB was achieved as the improvement of the SNR.

5. Conclusion

In this paper, the discrete wavelet transform denoising technique was successfully demonstrate on a Φ-OTDR sensing data for vibration detection. Even though the data involved for the purpose of obtaining a clear vibration detection was heavily impeded by noise, the proposed technique significantly diminished the said noise with desired preserved signals that aided the target of extracting and detecting the vibration point perfectly. There was equally a significant enhancement of the SNR value. In conclusion, the proposed denoising technique proved effective in enhancing the performance of the Φ-OTDR sensing in distributed vibration sensing.

References

[1] P. Wang, Shixin Lou, Sheng Liang, Y. Zhang, ”Selective average based threshold algorithm for Φ-OTDR distributed fifiber-optic sensing system”,Infrared and Laser Engineering, 45, 0322003 (2016).

[2] F. Peng, Han Wu, Xin-Hong Jia, Yun-Jiang Rao, Zi-Nan Wang, and ZhengPu Peng, ”Ultra-long high-sensitivity Φ-OTDR for high spatial resolution intrusion detection of pipelines”, Optics Express 22, 13804-13810 (2014).

[3] D. Chen, Qing wen Liu, And Zuyuan He, ”Phase-detection distributed fifiber-optic vibration sensor without fading-noise based on time-gated digital OFDR”, OPTICS EXPRESS 25, 8315 (2017).

[4] Z. Wang, Li Zhang, Song Wang, Naitian Xue, Fei Peng, Mengqiu Fan, Wei Sun, Xianyang Qian, Jiarui Rao, and Yunjiang Rao, ”Coherent Φ-OTDR based on I/Q demodulation and homodyne detection”, Optics Express 24, 853 (2016).

[5] Z. Wang, Bin Zhang, Ji Xiong, Yun Fu, Shengtao Lin, Jialin Jiang, Yongxiang Chen, Yue Wu, Qingyang Meng, Yunjiang Rao, ”Distributed acoustic sensing based on pulse-coding phase sensitive OTDR”, IEEE Internet of Things, 6, 6117-6124 (2019).

[6] Y. L. Lu, T. Zhu, L. A. Chen, and X. Y. Bao, ”Distributed vibration sensor based on coherent detection of phase-OTDR”, Lightw.Technol. 28, 3243-3249 (2010).

[7] Z. Pan, K. Liang, Q. Ye, H. Cai, R. Qu, and Z. Fang, ”Phase-sensitive OTDR system based on digital coherent detection”, Asia Communications and Photonics Conference and Exhibition, (Optical Society of America) 83110S (2011).

[8] F. Pang, M. He, H. Liu, X. Mei, J. Tao, T. Zhang, X. Zhang, N. Chen, and T. Wang, ”A fading-discrimination method for distributed vibration sensor using coherent detection of Φ-OTDR”, IEEE Photonics Technology. Letter 28, 2752-2755 (2016).

[9] G. Andria, F. Attivissimo,A.M.L. Lanzolla, and M. Savino, ”A Suitable Threshold for Speckle Reduction in Ultrasound Images”, IEEE Transactions on Instrumentation And Measurement, 62, 2270-2279 (2013).

[10] G. H.Wang, Li, D. H.; Pan, W. M.; Zang, Z. X., ”Modifified switching median fifilter for impulse noise removal”. Signal Process 90, 3213-3218 (2010).

[11] D.J. Jwo, T. S.Cho, ”Critical remarks on the linearised and extended Kalman fifilters with geodetic navigation examples”, Measurement 43, 1077- 1089 (2010).

[12] Zhu, X. Xiao, Q. He, and D. Diao, Enhancement of SNR and spatial resolution in phi-OTDR system by using two-dimensional edge detection method, Journal of Lightwave Technology, (2013), 31(17): 28512856.

[13] G. Hennenfent and F. J. Herrmann, Seismic denoising with nonuniformly sampled curvelets, Comput. Sci. Eng. (2006), vol. 8, no. 3, p. 16.

[14] B. Weng; Blanco-Velasco, M.; Barner, K.E. ECG denoising based on the empirical mode decomposition. In Proceedings of the 28th IEEE EMBS Annual International Conference, New York, NY, USA, (2006); pp. 14.

[15] M. Han; Y. Liu; Xi, J.; W. Guo, ”Noise smoothing for nonlinear time series using wavelet softthreshold”, IEEE Signal Process. Letter 14, 62-65 (2007).

[16] J. Baili; S. Lahouar; M. Hergli; I. L. Al-Qadi; K. Besbes, ”GPR signal de-noising by discrete wavelet transform”, NDT E. Int. 42, 696-703 (2009).

[17] H. F. Taylor and C. Lee, Apparatus and method for fifiber optic intrusion sensing, U.S. Patent 5194847, 1993.

[18] A. H. Hartog, An Introduction to Distributed Optical Fibre Sensors, 1st ed. (CRC Press, 2017).

[19] C. Lin and Liu A, Tutorial of the Wavelet Transform, February 23,2010.

[20] D.L. Donoho, I.M. Johnstone, G. Kerkyacharian, D. Picard, Wavelet shrinkage: Asymptopia?, J. Roy. Statist. Soc. 57 (1995) 301369.

[21] Rafael C. Gonzalez, Richard E.woods, Digital Image Processing, published by dorling Kindersley (india) Pvt.ltd, ISBN 81-7758-168-6.

[22] Atubga D.A.I,Shengtao L., Ji X., Jialin J.,1 Yun F., AND Zinan W. et. al.,Integrated principal component analysis denoising technique for phasesensitive optical time domain reflectometry vibration detection, Applied Optics, 59, 3 (2020)